INTERNATIONAL JOURNAL OF OPTIMIZATION IN CIVIL ENGINEERING
Int. J. Optim. Civil Eng., 2014; 4(2):187-205

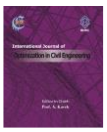

DYNAMIC PERFORMANCE OPTIMIZATION OF TRUSS STRUCTURES BASED ON AN IMPROVED MULTI-OBJECTIVE GROUP SEARCH OPTIMIZER

L.J. Li[*, †] and Z.H. Huang
School of Civil and Transportation Engineering, Guangdong University of Technology, Guangzhou, 510006, China

ABSTRACT

This paper presents an improved multi-objective group search optimizer (IMGSO) that is based on Pareto theory that is designed to handle multi-objective optimization problems. The optimizer includes improvements in three areas: the transition-feasible region is used to address constraints, the Dealer's Principle is used to construct the non-dominated set, and the producer is updated using a tabu search and a crowded distance operator. Two objective optimization problems, the minimum weight and maximum fundamental frequency, of four truss structures were optimized using the IMGSO. The results show that IMGSO rapidly generates the non-dominated set and is able to handle constraints. The Pareto front of the solutions from IMGSO is clearly dominant and has good diversity.

Received: 20 March 2014; Accepted: 10 June 2014

KEY WORDS: improved group search optimizer, multi-objective optimization, dynamic performance, truss structure

1. INTRODUCTION

In recent years, dynamic optimization, such as optimizing the properties of structural systems [1], has been used in structural engineering to efficiently control the dynamic response of structures. The main studies of structural dynamic optimization have focused on dynamic property optimization [2-4] and dynamic response optimization [5, 6]. In optimizing the

[*]Corresponding author: L.J. Li, School of Civil and Transportation Engineering, Guangdong University of Technology, Guangzhou, 510006, China
[†]E-mail address: lilj@gdut.edu.cn (L.J. Li)

dynamic properties of a structural design, researchers primarily consider the stiffness, classical damping, weight, natural frequencies and modes of the system as constraints or objectives. Many studies have considered the natural frequencies of a building as constraints or objectives; such buildings contain trusses, frames, shells and beams, which have simple constructions and clear interactions between elements [4, 7]. Dynamic response optimization considers factors such as the amplitude of vibration, velocity, acceleration, and stress and strain. Dynamic response optimization is more difficult than dynamic property optimization because the objective functions are more complex.

Multi-objective optimization problems [8], whose solutions have to be searched for in feasible regions of designs for all fitness functions and constraints, are much more similar to practical engineering problems. A multi-objective optimization problem can be solved by converting it to a single-objective problem; however, because the solving method has strict demands on the fitness functions, it cannot efficiently be used for practical engineering. Many efficient multi-objective algorithms based on Pareto-optimal fronts have emerged in recent years; among these, genetic algorithms [9-11] and particle swarm optimizers [12-14] for multi-objective optimization have been studied by many researchers and are utilized widely. The deficiencies of genetic algorithms are their low search efficiencies, slow convergence speeds and their tendency to fall into locally optimal solutions. The disadvantage of the particle swarm optimizer is that it is time consuming because of its search strategy. The group search optimizer (GSO) [15, 16], which is inspired by the behavior of animals, has been successfully applied to optimal structural design [17-19]. In particular, the multi-objective group search optimizer (MGSO), which is based on GSO, has been used to solve optimization problems with multiple objectives. However, research has mostly focused on static property optimization, and dynamic optimization can be improved greatly.

The aim of this paper is to propose an improved multi-objective group search optimizer (IMGSO) that is based on MGSO and can be used for structural multi-objective optimization. The first natural frequency (fundamental frequency) and the weight of the structure are considered as the two main objectives of the optimization. This paper analyzes the capability and applicability of IMGSO for the multi-objective dynamic optimization of truss structures.

2. GROUP SEARCH OPTIMIZER (GSO)

The group search optimizer (GSO), which is based on the producer-scrounger model proposed by biologists, contains three searching group members, the producer, scrounger and ranger, and each member has different functions [15]. The producer and scroungers are the key members for searching and are the basis of the producer-scrounger model, while the ranger is used in GSO to avoid entrapment in locally optimal solutions and performs random walks around the entire search region. The producer is the individual with the best fitness value (under the current conditions). At the end of each iteration, the GSO program chooses one individual as the producer based on the best fitness value. Scroungers then join the resource found by the producer to randomly find a better solution around the producer. Finally, rangers move over the entire search space.

In an n-dimensional search space, the ith member in the kth iteration has a current position $X_i^k \in R^n$, a head angle $\varphi_i^k = (\varphi_{i1}^k, ..., \varphi_{i(n-1)}^k) \in R^{n-1}$ and a direction

$D_i^k(\varphi_i^k) = (d_{i1}^k, ..., d_{in}^k) \in R^n$. In each interaction, each member in the group performs in the following manner.

The producer scans at zero degrees and then scans laterally by randomly sampling three points in the scanning field at zero degrees, the left side and the right side according to equations (1), (2) and (3), respectively. The scroungers follow the producer and walk toward it randomly according to equation (4). Rangers move over the search space randomly. If the ith member in the kth iteration is chosen as a ranger, it will choose a random head angle and distance based on equations (5) and (6), respectively, and walk toward the new position based on equation (7).

$$X_z = X_p^k + r_1 l_{\max} D_p^k(\varphi^k) \tag{1}$$

$$X_l = X_p^k + r_1 l_{\max} D_p^k(\varphi^k - r_2 \theta_{\max}/2) \tag{2}$$

$$X_r = X_p^k + r_1 l_{\max} D_p^k(\varphi^k + r_2 \theta_{\max}/2) \tag{3}$$

$$X_i^{k+1} = X_i^k + r_3(X_p^k - X_i^k) \tag{4}$$

$$\varphi^{k+1} = \varphi^k + r_2 \alpha_{\max} \tag{5}$$

$$l_i = a \cdot r_1 l_{\max} \tag{6}$$

$$X_i^{k+1} = X_i^k + l_i D_i^k(\varphi^{k+1}) \tag{7}$$

Where $r_1 \in R^1$ is a normally distributed random number with a mean of 0 and a standard deviation of 1; $r_2 \in R^{n-1}$ is a random sequence in the range (0, 1), and $r_3 \in R^n$ is a uniform random sequence in the range (0, 1).

An essential difference between multi-objective optimal problems and single-objective optimal problems is that a result of the former is a set of solutions or groups of sets, while the result of the latter is one solution or one set of solutions. However, the successful implementation of GSO to solve a single-objective optimal problem [14, 15] does not necessarily illustrate its effectiveness for multi-objective optimal problems.

3. MULTI-OBJECTIVE GROUP SEARCH OPTIMIZER (MGSO)

The multi-objective group search optimizer (MGSO) proposed by Li et al. [20] is based on the GSO. The major difference between MGSO and GSO is the comparison rule of the fitness values. MGSO sorts each member to generate the non-dominated set by the members' non-dominated ranks and crowded distance and then chooses a member from the non-dominated set as a producer in each interaction. The merits and demerits of MGSO are as follows:

1. The crowded-comparison operator [11] is used to simply and conveniently guide members in each interaction to obtain uniformly-spread Pareto optimal front solutions. However, this ability of the operator declines gradually after each interaction, so suitable operators should be considered during the rest interactions and especially approaching the

maximum interaction.

2. MGSO chooses the member with an infinite crowding distance as the producer, which is normally distributed at the two ends of the Pareto front. The advantages of doing this are that it is easy to converge to a widely spread-out but non-uniform Pareto front. However, the disadvantages are that non-dominate solutions concentrate near the extreme solutions and thus form a non-uniform distribution of non-dominate solutions.

3. To handle the given constraints, MGSO uses a method of multiplication by a large number. Whenever a member violates the constraints, its fitness values are assigned to *inf* or *zero* for the maximum or minimum optimal problem, respectively. The feasible solutions dominate the infeasible solutions. Thus, all of the infeasible solutions are ignored, including the infeasible solutions that are close to boundaries, but they may be useful.

4. Repeated comparisons, or comparing non-dominated members generated at every interaction, is used by MGSO to update the non-dominated external archive or the Pareto non-dominated set. Consequently, the required computational time is increased.

4. IMPROVED MULTI-OBJECTIVE GROUP SEARCH OPTIMIZER (IMGSO)

This paper describes three improvements to MGSO: choosing the producer, handling constraints and updating the non-dominated external archive.

4.1 Transition-feasible region

Handling constraint suitably is a technical aspect of solving constrained optimization problems. In the literature of constrained optimization problems, optimal solutions are always distributed near or on the constrained boundary. If this condition is not true, then the constraints do not work or do not work efficiently. Under this condition, the results are not closely related to the constraints. For some problems, the fitness value of an infeasible solution may be better than that of the feasible solution. In fact, the feasible solution, which lies around an infeasible solution near the feasible region, exists even if the researcher does not have enough information to find it. Consequently, it is more practical and convenient to search for a globally optimal solution using information about an infeasible solution than by comparing feasible solutions; this is especially true for algorithms that are based on GSO. Based on the analysis presented above, an improved GSO with the transition-feasible region is presented and is shown in Fig. 1.

Definition 1: The distance [21] between an arbitrary point x and the feasible region F is defined as

$$d(x,F)=\sum_{i=1}^{m}\max\{0,k_i(x)\} \qquad i=1,2,\cdots,m \tag{8}$$

where $k_i(x)$ is the *ith* constraint function; whenever point x satisfies this function, then $k_i(x)\le 0$ or $k_i(x)>0$. Obviously, the relationship between point x and the feasible region F is

the same as the following expression:

If $d(x,F)=0$ *then* $x \in F$ *otherwise* $x \notin F$

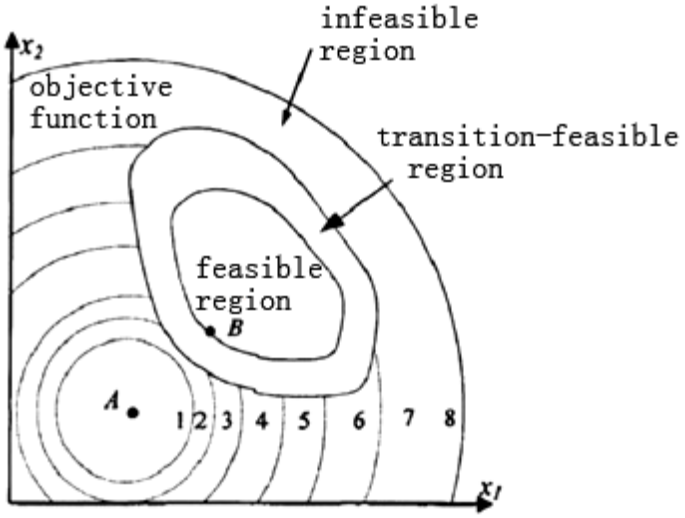

Figure 1. The transition-feasible region

Definition 2: For a given positive constant ε ($\varepsilon \in R^+$), region *H*, which satisfies $0 < d(x,F) < \varepsilon$, is the transition-feasible region, and ε is called the transition-feasible width. Solutions that are distributed in the region *H* are defined as the transition-feasible solutions.

The transition-feasible solutions can be chosen by the objective function or by comparison of Pareto dominance together with the feasible fitness values. The main use of the transition-feasible region is to ensure that the producer is chosen from either the feasible or transition-feasible region. For a producer that controls the iteration direction of GSO, the producer assures the correctness of the evolutionary direction. The analysis presented above concludes as follows: (1) in the case of a feasible region that is much smaller than the entire search space, it is faster to use the transition-feasible solutions to search for feasible solutions in separate directions and is easy to converge to the Pareto front, especially for transition-feasible solutions with lower $d(x,F)$; (2) the transition-feasible solutions may help to find the globally optimal solution if the true Pareto-optimal front is near the feasible boundary.

Due to the infeasibility of transition-feasible solutions, the Pareto non-dominated set will be infeasible when transition-feasible solutions are included. A measure that can filter transition-feasible solutions out of the external elite set is taken whenever the interaction reaches certain points, which can make full use of the transition-feasible information. On the other hand, the final solutions, which are filtered several times, are all feasible and are distributed uniformly.

4.2 Building a non-dominated set using the Dealer's Principle

Most of the studies on multi-objective optimal design are based on Pareto-optimal solutions. The non-dominated set is adjusted by repeatedly maintaining and updating it to achieve the

true Pareto-optimal front. Within the non-dominated set, the best members are evaluated by the crowded-comparison operator of Pareto. The non-dominated set is a locally optimal set before converging. The main procedure of multi-objective algorithm convergence can be summarized as follows: (1) randomly generate the initial members; (2) construct or update all of the members of the non-dominated set based on the crowded-comparison operator [8]; (3) generate the new members in each iteration using the evolutionary mechanism; (4) combine the new members and old members; (5) repeat steps (2) to (4) until the convergence criterion is met. Thus, the critical technique of Pareto-optimal set construction is step (2). The procedure described in this paper replaces the crowded-comparison operator with the Dealer's Principle [22] to reduce the computational time.

The Dealer's Principle is a non-backtracking method. New non-dominated solutions are only generated by the current generation; a comparison of the current generation with the current non-dominated set is not needed. The current generation is copied to a temporary set *Q* before adding any new non-dominated members. A dealer, which is randomly chosen from *Q* and deleted from *Q* at the same time, will compare the remaining members in *Q* based on the domination relationship. If the dealer dominates some members in the current *Q*, those members will be canceled; if the dealer is not dominated, it will join the non-dominated set. These operations repeat until *Q* is empty. The procedure of generating the non-dominated set for the current generation *P* can be summarized as follows:

Construct a temporary set *Q*; originally, *Q=P*. Initialize the non-dominated set *NDSet*; originally, *NDSet=Ø;*

Choose a member *X* from *Q*, modify *Q* as *Q=Q-{X}*, and reset the dominated set *DSet=Ø* ;

Make $DSet = DSet\{Y \mid X \succ Y, \forall Y \in Q\}$;

Make *Q=Q-DSet*; if $\exists Z \in Q$ is untrue, then $Z \succ X$, $NDSet = NDSet \bigcup \{X\}$;

Repeat steps (2) to (4) until *Q* is empty.

4.3 Selection of the producer

The members of the non-dominated external archive are candidates for the producer (the global best individual). The producer is chosen from the archive and has great influence on the updating of the generation, the solution's diversity and the globally optimum convergence. It is important to utilize a reasonable method to choose the producer, which will guide the entire evolutionary direction, determine a much better spread of solutions and ultimately obtain better convergence near the true Pareto-optimal front.

In this paper, a producer is selected using a hybrid mechanism that consists of a tabu search and a crowded distance operator. In the earlier interaction, members with *inf* crowding distances are selected from the non-dominated external archive to play the role as producer and extend the diversity of the archive. The archive then gradually becomes spread-out and uniform but is not close enough to the true Pareto-optimal front. A tabu search is utilized in the latter interaction.

The memory function of the tabu search is performed using a tabu list, which records the members chosen as producers when the latter interaction begins. An essential point is that whenever a member is selected as a producer candidate, the member will not be selected

again in later interactions; thus, the producers will not be the same at any one time. Because of its stochastic nature, an intelligent algorithm may converge to the local optimum. To prevent this from happening, the producer performs a novel evolutionary direction and leads the generation to a search space that has not been used before. This provides more equal opportunities for all of the members in the non-dominated external archive to be chosen and keeps the External Elite Set (EES), which is trimmed by the non-dominated external archive, much closer to the true Pareto-optimal front in each interaction.

4.4 External Elite Set

In the multi-objective optimal problem, because the true Pareto-optimal front may be extensive and have an infinite number of members, it is unnecessary to present all non-dominated solutions. A reasonable way is to collect representative members into the EES, which is an external archive with a maximum capacity of *N*. These members have excellent convergence, uniformity and diversity. The members from the non-dominated external archive are inserted into the EES based on their traits in each interaction. By continually maintaining and updating the EES, the last EES is the final optimal solution set.

The EES converges to the true Pareto-optimal front by eliminating dominated solutions in EES based on the dominated relationship of the Pareto solutions. Several general methods [13] can fulfill this requirement, including information entropy, adaptive grid and crowding-distance calculation methods. This study adopted the crowding-distance calculation method to maintain the EES. As shown in Fig. 2, members with smaller crowding distances have greater crowding densities.

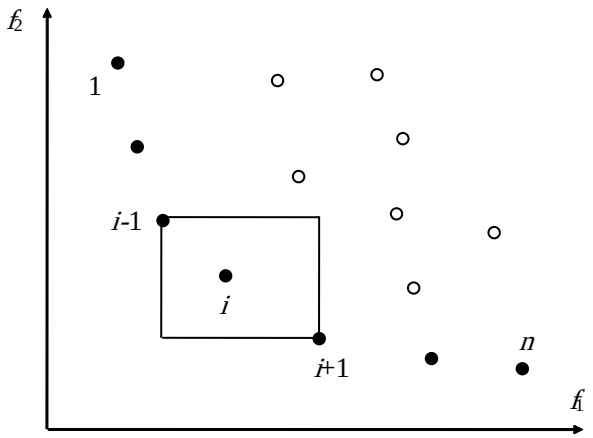

Figure 2. Diagram of crowding distance

As shown in Fig. 2, f_1 and f_2 are two objectives of the problem. The crowding distance of the *ith* member is half the perimeter of the rectangle. Suppose $P[i]_{distance}$ is the crowding distance of the *ith* member, and $P[i].m$ is the fitness value of member *i* for objective *m*. Then:

$$P[i]_{distance} = (P[i+1].f_1 - P[i-1].f_1) + (P[i+1].f_2 - P[i-1].f_2) \quad (9)$$

Generally, for *r* objectives, the crowding distance of the *ith* member can be expressed as:

$$P[i]_{distance} = \sum_{k=1}^{r} (P[i+1].f_k - P[i-1].f_k) \quad (10)$$

A greater distance of a member from its surrounding members means it has a lower crowding density and vice versa. The use of the crowding distance can be summarized as:

Determine the maximum capacity *n* for EES;

For every EES member *i*, initialize its crowding distance as $P[i]_{distance} = 0$;

Sort the *mth* fitness value of the *ith* member by their fitness values in ascending order, namely $I = sort(i, m)$;

The distance of the members, especially the first and the last in the order sorted in step (3), is set to infinity; namely $P[1]_{distance} = P[n]_{distance} = \infty$;

For the members that are from *2nd* to *(n-1)th* in order, the crowding distance is calculated by (11) as:

$$P[i]_{distance} = P[i]_{distance} + \frac{P[i+1].m - P[i-1].m}{f_m^{\max} - f_m^{\min}} \quad (11)$$

(6)Return to step (3) and repeat until the crowding distance calculations are complete for all members.

4.5 Improved multi-objective group search optimizer (IMGSO)

IMGSO utilizes the EES to store the non-dominated set, uses the transition-feasible region to handle constraints and sets a feasible filter to ensure that the final Pareto-optimal solutions are feasible. Adoption of the Dealer's Principle reduces the comparative frequency and enhances the efficiency with less computational time. The hybrid mechanism that combines a tabu search and the crowded distance operator is a reasonable method to choose the producer, which allows the generation to evolve in the latter interactions and improves the diversity.

IMGSO includes three different groups: the searching group based on GSO, the non-dominated set in each interaction and the EES, which reserves excellent members. The operations and relationships between the three groups are shown in Fig. 3.

When the procedure starts running, it initializes the population randomly and constructs the current non-dominated set based on the current population. It should be noted that the non-dominated set includes members that are generated by the current population based on Pareto dominance. The EES is a limited set that includes excellent members or representative members from the non-dominated set. To attain a uniformly spread-out EES, members of the non-dominated set are inserted into the EES to maintain and update it. At the end of the procedure, the EES is output. As mentioned previously, the members of the

EES are chosen as producers using a reasonable measure, and the producer will then guide the population to evolve in the next interaction.

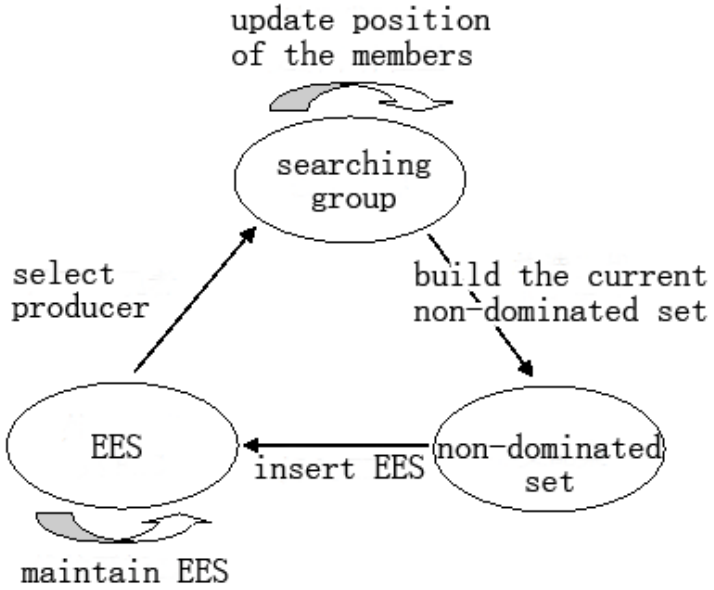

Figure 3. Relationships between three groups of IMGSO

4.6 IMGSO optimization procedure

Based on the technique described above, the IMGSO process can be described as follows:

I. Initialize the positions and head angles of all of the members randomly.

II. Determine the transition-feasible width ε; evaluate the fitness function of the current population; construct the non-dominated set by Pareto dominance; calculate the crowding distance and sort members in a certain order; select members as producers by the greatest crowding distance.

III. Build an external non-dominated set and an EES to manage the non-dominated solutions. The maximum capacities of the external non-dominated set and the EES are *inf* and *M*, respectively. The former stores all of the non-dominated solutions, while the latter stores the best solutions as *M*.

IV. Producer's search behavior:

1. First scan at zero degrees; then, three points at zero degrees, the left side and right side are checked using equations (1), (2) and (3), respectively;
2. Check if any dimensions cross the boundary of the variables, then replace the bad dimensions by the primary dimension of the producer (fly-back mechanism);
3. Compare the three new positions with the primary position based on Pareto dominance; eliminate the dominated positions and keep the non-dominated positions.

Scrounger's search behavior: 80% of the rest group members are randomly selected as scroungers. The scroungers will conduct a uniform search around the producer using equation (4).

Ranger's search behavior: the remaining group members are introduced as rangers,

which walk randomly in the search space. First, generate a random head angle using equation (5), then choose a random distance from the Gaussian distribution using equation (6), and finally move to the new point using equation (7).

V. Check all of the members to determine if any dimension crosses the boundary of the variables, then replace the bad dimension based on the fly-back mechanism.

VI. Evaluate the fitness functions for the current group members, reconstruct the non-dominated set and maintain the EES, and choose a new producer based on the method described in section 3.3.

VII. Stop the procedure if the stopping criterion is fulfilled; otherwise go to step (iv).

5. MATHEMATICAL MODEL AND NUMERICAL EXAMPLES

5.1 Multi-objective dynamic performance optimization problem

The variables of the multi-objective dynamic properties for truss structures are the frame sections. The multi-objective problem considers the minimum weight and the maximum fundamental frequency. The constraints of the problem are based on the frame stress and the joint displacement. The mathematical model is shown as:

$$\begin{aligned} &\min.\ f_1 = W = \sum_{i=1}^{m} \rho_i A_i L_i \\ &\max.\ f_2 = \omega \\ s.t.\quad &g_n(A, X) \le 0 \ \ (n = 1,2,\cdots, n_G); \\ &A_i \in S = \{S_1, S_2, \cdots, S_{n_e}\} \ \ (i = 1,2,\cdots, m); \\ &X_k^{\min} \le X_k \le X_k^{\max} \ \ (k = 1,2,\cdots, n_c) \end{aligned} \tag{12}$$

where f_1 and f_2 are two objective functions; W is the weight of the structure; ω is the fundamental frequency; $A = [A_1, A_2, \cdots, A_m]^T$ represents m variables of the frame section area with either continuous variables or discrete variables; $X = [X_1, X_2, \cdots, X_{n_c}]^T$ represents n_c variables of the joint displacement, which are continuous variables; $g_n(A, X)$ are n_G deterministic constraints of stress and displacement; $S = \{S_1, S_2, \cdots, S_{n_e}\}$ is a given set of discrete values for the section area; $X_k^{\min}$ and $X_k^{\max}$ are the lower and upper bounds, respectively; and ρ_i and L_i are the density and the length of the frame elements, respectively.

In this study, the structural analysis is performed using Matlab and ANSYS. The main optimization process is written in Matlab, and the static analysis and calculations of the natural frequencies are performed by functions in ANSYS.

5.2 Numerical examples

1. The 10-bar plane truss structure

The 10-bar plane truss structure is shown in Fig. 4. Specific details about the geometry, material and load case can be found in reference [4]. The design variables are the frame section areas, which are discrete variables. Stress and displacement are considered as constraints. The maximum capacity of the EES is 30, the size of the population is 300, and the transition-feasible width ε is one-tenth of the allowable stress. IMGSO and MGSO [4] perform 50 iterations and 100 iterations, respectively. The solutions are shown in Fig. 5 and Fig. 6.

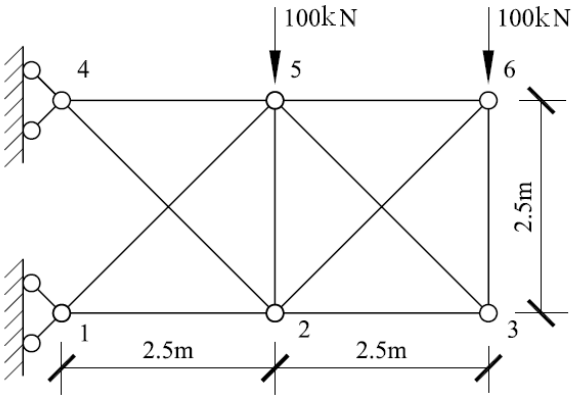

Figure. 4 The 10-bar plane truss structure

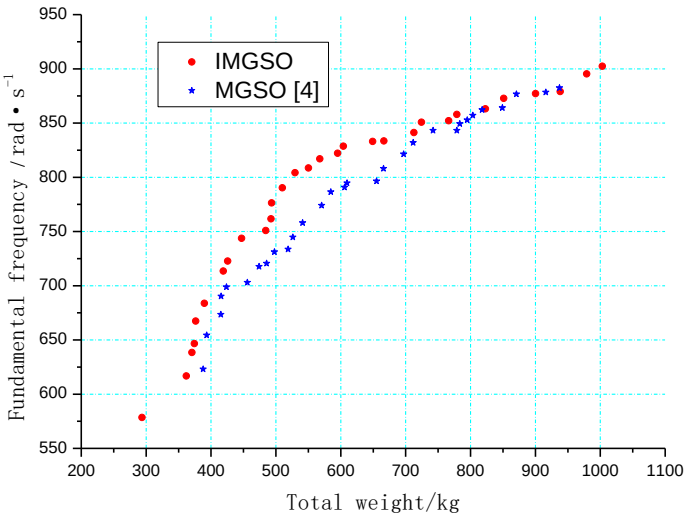

Figure. 5 Results of the EES after 50 iterations

As shown in Fig. 5, the non-dominated set of IMGSO almost always dominates that of MGSO; this dominance is clear in the middle of the non-dominated set and illustrates that

the selection of the producer works effectively in the earlier interactions. The EES of IMGSO is more uniform than that of MGSO. However, the uneven curves indicate that it may converge to a better Pareto-optimal curve by continuously maintaining the EES based on the measure presented in this paper.

The extreme solution of IMGSO after 50 interactions for (*maxW*, *max* ω) is (1003.1181 *kg*, 902.4423 *rad/s*), and the extreme solution for (*minW*, *min* ω) is (293.6646 *kg*, 578.4806 *rad/s*). The ranges of the weight and the fundamental frequency are 293.6646 *kg*≤*W*≤1003.1181 *kg* and 578.4806 *rad/s*≤ω≤902.4423 *rad/s*, respectively.

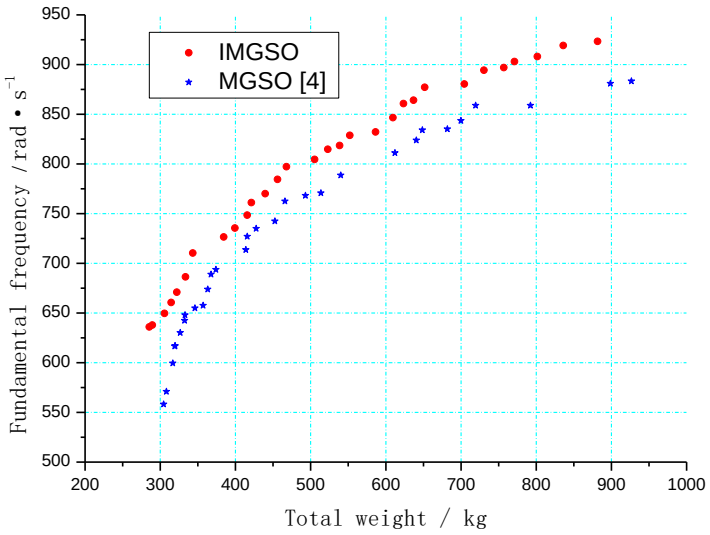

Figure. 6 Results of the EES after 100 iterations

Fig. 6 shows that the non-dominated set of IMGSO completely dominates that of MGSO after 100 interactions. The dominance is superior to that shown in Fig. 5 and is improved even for solutions near the extreme solutions. It should be noted that the search ability of IMGSO is still effective in the latter interactions. IMGSO is effective in dealing with the constraints. The mechanism that handles constraints also demonstrates that the transition-feasible region helps to find better non-dominated solutions.

The extreme solution of IMGSO after 100 interactions for (*maxW*, *max* ω) is (881.6371 *kg*, 923.3845 *rad/s*), and the extreme solution for (*minW*, *min* ω) is (285.4306 *kg*, 636.0439 *rad/s*). The ranges of the weight and the fundamental frequency are 285.4306 *kg*≤*W*≤881.6371 *kg* and 636.0439 *rad/s*≤ω≤923.3845 *rad/s*, respectively. Fig. 5 and Fig. 6 show that the range of 100 interactions is larger than that of 50 interactions; this is because the former is closer to the true Pareto-optimal front than the latter is. The range of solutions of the former represents the range of the true Pareto-optimal front.

The result of IMGSO, which is better than that of MGSO, illustrates the advantage of IMGSO in dynamic performance optimizations. Unlike the single-objective optimization algorithm, the multi-objective optimization algorithm searches the non-dominated set for

the minimum weight and the maximum frequency, which provides more possible solutions as a compromise for the final design scheme.

2. The 40-bar plane truss structure

The 40-bar plane truss structure is shown in Figure 7. Specific details about the geometry, material and load case can be found in reference [4]. Because of the large number of design variables, the maximum capacity of the EES is *inf*, which means that the EES is the same as the non-dominated set. The size of the population is 300, and the transition-feasible width ε is the sum of one-tenth of the allowable stress and one-fifth of the allowable displacement. Both IMGSO and MGSO [4] perform 50 iterations. The optimal results are shown in Fig. 8.

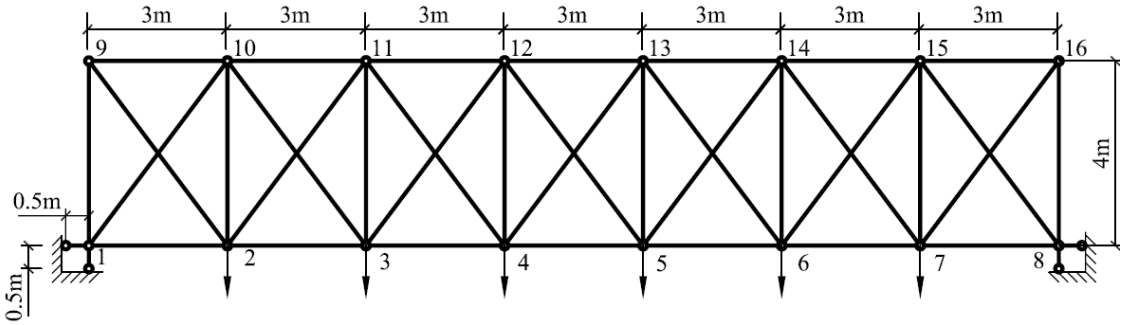

Figure. 7 The 40-bar plane truss structure

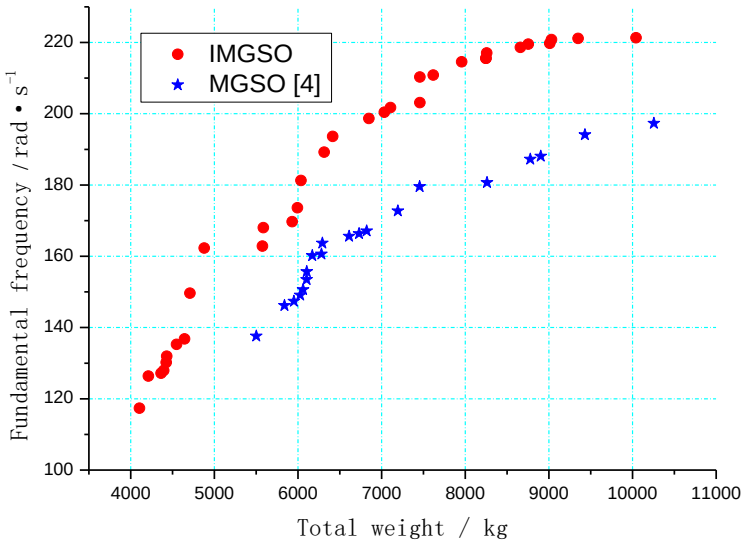

Figure. 8 Results of the EES after 50 iterations

As shown in Fig. 8, the non-dominated set of IMGSO completely dominates that of MGSO after 50 interactions, and IMGSO attains 34 non-dominated solutions, while MGSO

attains 21. MGSO utilizes a death penalty to handle constraints. If a member violates the constraints, its fitness values will be assigned to *inf*, which ignores any available information from infeasible solutions. However, IMGSO reuses these infeasible solutions by introducing the transition-feasible region and thus attains more feasible solutions than MGSO does.

Reference [4] did not provide the result of 100 interactions. When MGSO was used to run 100 interactions in reference [4], there was no apparent improvement of the results, which illustrates that MGSO is not practical for solving complex multi-constraint optimization problems. Figure 8 shows that the non-dominated set of IMGSO is complex and that the curve is uneven after 50 interactions. It should be noted that the non-dominated set is still far from the true Pareto-optimal front. The optimal results of IMGSO after 100 and 50 interactions are shown in Fig. 9.

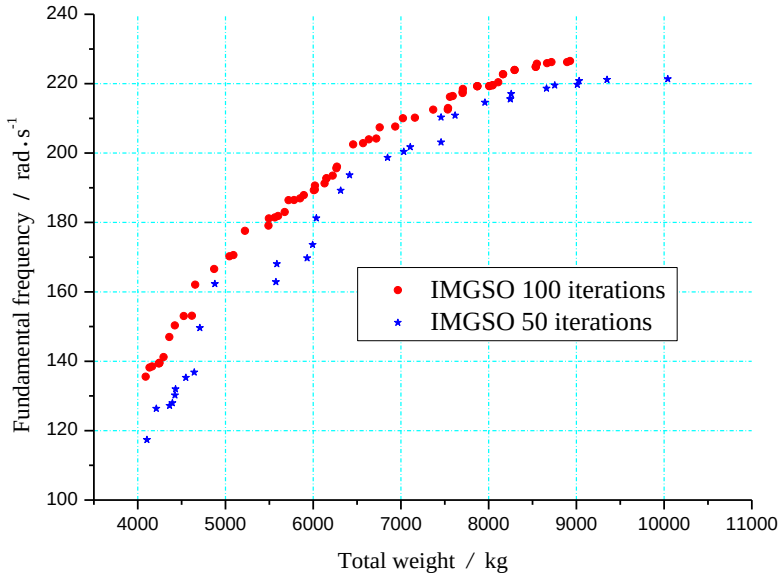

Figure 9. Comparison of the results of the EES after 100 iterations and 50 iterations

Fig. 9 shows that the non-dominated set of IMGSO after 100 interactions dominates the set after 50 interactions. The former obtains 69 non-dominated solutions, and the latter obtains 34. The non-dominated set approaches the true Pareto-optimal front as the number of interactions increases. The non-dominated curve, which is composed of the discrete solutions, is uniform and smooth after 100 interactions, which indicates that the solution is much closer to the true Pareto-optimal front

The extreme solution of IMGSO after 100 interactions for (*maxW*, *max* ω) is (8927.3265 *kg*, 226.5194 *rad/s*), and the extreme solution for (*minW*, *min* ω) is (4090.5623 *kg*, 135.5479 *rad/s*). The ranges of the weight and the fundamental frequency are 4090.5623 *kg*$\leq W \leq$8927.3265 *kg* and 135.5479 *rad/s*$\leq \omega \leq$226.5194 *rad/s*, respectively. A compromise

solution based on the Euclidean distance is chosen as (5222.1442 *kg*, 177.5935 *rad/s*).

3. The 15-bar spatial truss structure

The 15-bar spatial truss structure is shown in Fig. 10. Specific details about the geometry, material and load case can be found in reference [4]. The size of the population is 300, and the maximum capacity of the EES is *inf*. The IMGSO and MGSO [4] perform 50 and 100 iterations, respectively. The results are shown in Figs. 11 and 12.

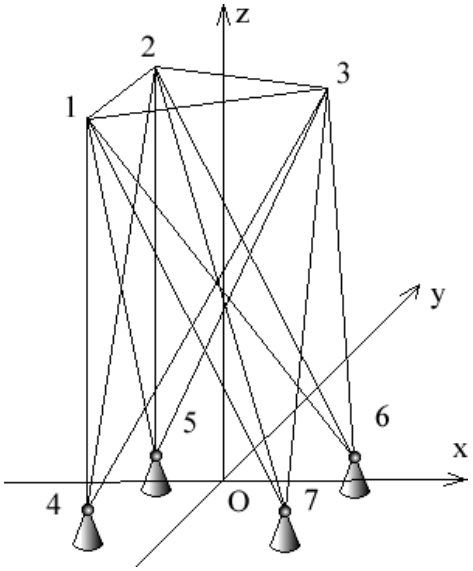

Figure. 10 The 15-bar spatial truss structure

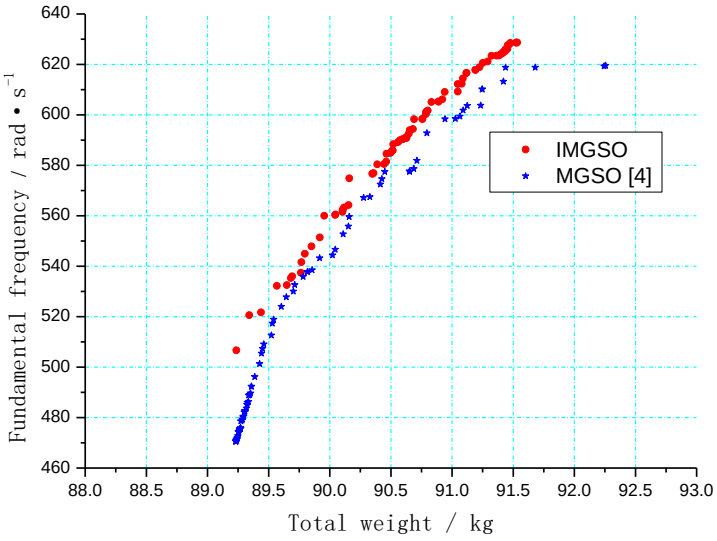

Figure. 11 Results of the Pareto front after 50 iterations

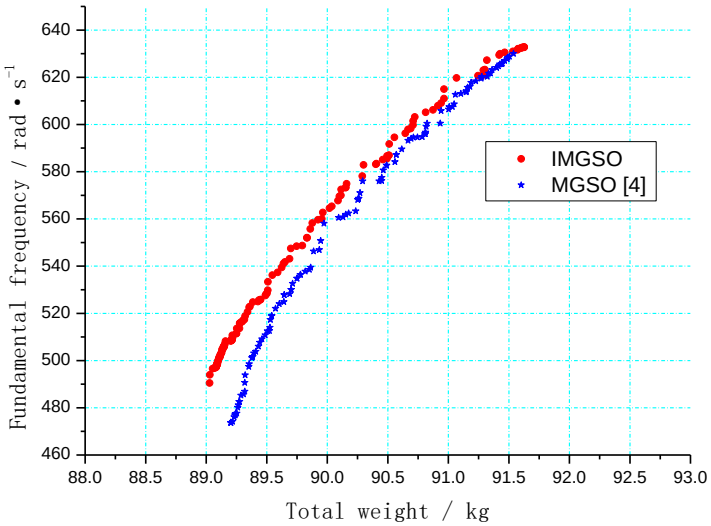

Figure. 12 Results of the Pareto front after 100 iterations

As shown in Fig. 11 and Fig. 12, the non-dominated sets of IMGSO dominate those of MGSO after 50 and 100 interactions, respectively. The dominance of IMGSO improves after 100 interactions. IMGSO attains 140 non-dominated solutions, which is slightly more than the 122 attained by MGSO. The advantage of IMGSO is clear in the earlier interactions. However, the effectiveness of the constraint handling is not as apparent. This case demonstrates that the superiority of IMGSO in dynamic property optimization will improve when the number of interactions increases.

4. The 25-bar spatial truss structure

The 25-bar spatial truss structure is shown in Fig. 13. Specific details about the geometry, material and load case can be found in reference [4]. The size of the population is 300, and the maximum capacity of EES is *inf*. The IMGSO and MGSO [4] perform 50 and 100 iterations, respectively. The results are shown in Figs. 14 and 15.

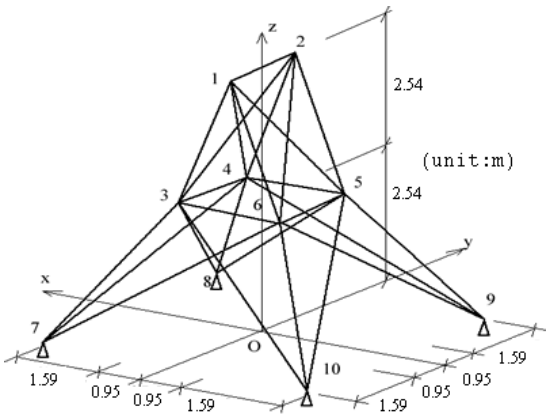

Figure 13. The 25-bar spatial truss structure

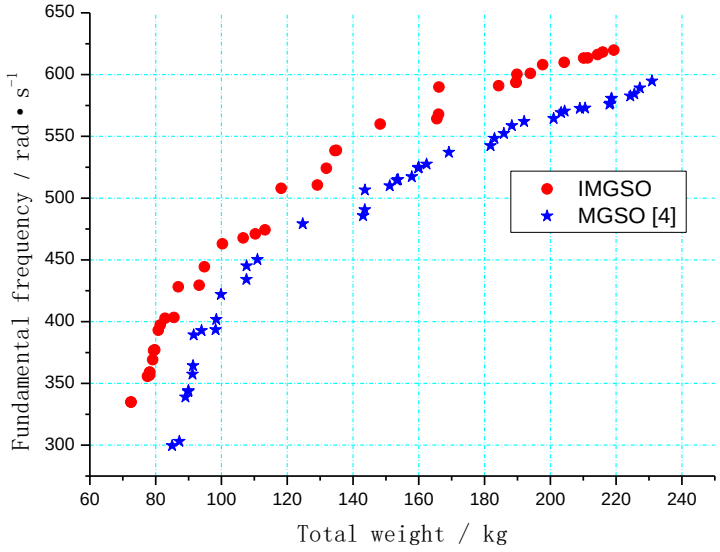

Figure 14. Results of the Pareto front after 50 iterations

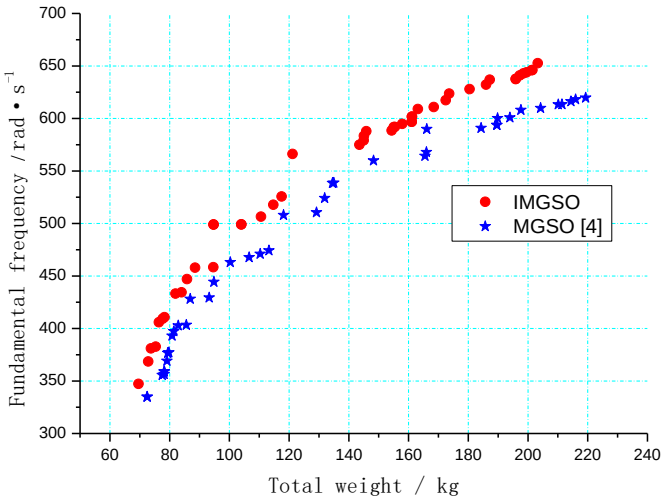

Figure 15. Results of the Pareto front after 100 iterations

As shown in Fig. 14 and Fig. 15, the non-dominated sets of IMGSO completely dominate those of MGSO after 50 interactions and 100 interactions, respectively. The superiority of IMGSO shown in Fig. 15 is not as good as that shown in Fig. 14. Its dominance is still apparent after 100 interactions, and IMGSO attains 48 non-dominated solutions, while MGSO attains 46 solutions. Fig. 15 shows that the non-dominated curve is not smooth, which indicates that IMGSO has the potential for further evolution. The result after 200 interactions is shown in Fig. 16.

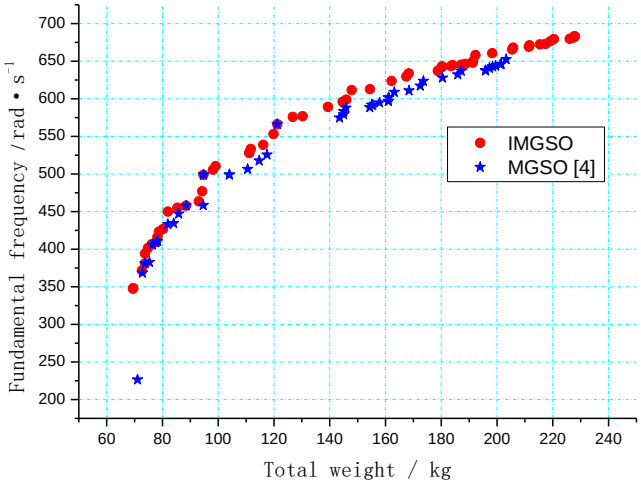

Figure16. Results of the Pareto front after 200 iterations

As shown in Fig. 16, the non-dominated solutions of IMGSO can form smooth and uniform curves. Although the superiority decreases, it is obvious that the non-dominated curve of IMGSO dominates that of MGSO. The number of non-dominated solutions of IMGSO is greater than that of MGSO.

6. CONCLUSIONS

Four truss structures were examined for multi-objective optimization of the minimum weight and maximum fundamental frequency. The results of the optimizations show that IMGSO is a rapid search algorithm that finds non-dominated solutions using fewer generations than other methods. IMGSO shows clear dominance over MGSO after 50 interactions and has a good distribution, which demonstrates the effectiveness and superiority of IMGSO in handling constraints. Based on examples of two plane truss structures and two spatial truss structures, IMGSO is better in dealing with multi-dimensional variables and multiple constraints when solving complex problems. The results show that IMGSO is an efficient, practical multi-objective optimizer for the structural optimization of trusses.

ACKNOWLEDGEMENTS

This work was funded by the National Natural Science Foundation of China (Project No: 51178121, 51108188, 51208116) and the Natural Science Foundation of Guangdong Province (Project No: S2012020011082, 9151009001000059).

REFERENCES

1. Kaveh A, Farahmand Azar B, Hadidi A, Rezazadeh Sorochi F, Talatahari S. Performance-based seismic design of steel frames using ant colony optimization, *J Constr Steel Res* 2010; **66**(4): 566-574.
2. Li LJ, Xie ZH, Guo YC, Liu F. Structural optimization and dynamic analysis for double-layer spherical reticulated shell structures, *J Constr Steel Res* 2006; **62**(10): 943-949.
3. Kim H, Querin OM, Steven GP. On the development of structural optimization and its relevance in engineering design, *Design Studies* 2002; **23**(1): 85-102.
4. Li LJ, Liu F. *Group search optimization for applications in structural design*, Springer Berlin/Heidelberg, 2011.
5. Doğan E, Saka MP. Optimum design of unbraced steel frames to LRFD–AISC using particle swarm optimization, *Adv Eng Softw* 2012; **46**(1): 27-34.
6. Sergeyev O, Mroz Z. Sensitivity analysis and optimal design of 3D frame structures for stress for stress and frequency constraints. *Comput Struct* 2000; **75**(2):167-185.
7. Wang D, Zhang WH, Jiang JS. Truss optimization on shape and sizing with frequency constraints, *AIAA Journal* 2004; **42**(3): 622-630.
8. Deb K, Agrawal S, Pratap A, Meyarivan T. A fast elitist non-dominated sorting genetic algorithm for multi-objective optimization: NSGA II, *IEEE Trans Evol Comput* 2002; **6**(2), 182-197.
9. Johnston MD. An evolutionary algorithm approach to multi-objective scheduling of space network communications, *Intell Autom Soft Comput* 2008; **14**(3): 367-376.
10. Valli P, Antony Jeyasehar C. Genetic algorithm based equipment selection method for construction project using MATLAB tool, *Inter J Optim Civil Eng* 2012; **2**(2): 235-246.
11. Konak A, Coit DW, Smith AE. Multi-objective optimization using genetic algorithms: A tutorial, *Reli Eng Syst Safety* 2006; **91**(9): 992–1007.
12. Reyes-Sierra M, Coello C. Multi-objective particle swarm optimizers: A survey of the state- of-the-art, *Int J Comput Intell Res* 2006; **2**(3): 287-308.
13. Ray T, Liew K. A swarm metaphor for multiobjective design optimization, *Eng Optimz* 2002; **34**(2): 141-153.
14. Coello CAC, Pulido GT, Lechuga MS. Handling multiple objectives with particle swarm optimization, *IEEE Trans Evol Comput*, 2004; **8**(3): 256–279.
15. Li LJ, Xu XT, Liu F. The group search optimizer and its application to truss structure design, *Adv Struct Eng*, 2010; **13**(1): 43-51.
16. He S, Wu QH. A novel group search optimizer inspired by animal behavior. *2006 IEEE Congress on Evolutionary Computation*, Sheraton, 2006, pp. 4415-4421.
17. He S, Wu, QH, Sauders JR. Group search optimizer-an optimization algorithm inspired by animal searching behavior, *IEEE Trans Evol Comput*, 2009; **13**(5): 973-990.
18. Zeng SK, Li LJ. The particle swarm group search optimization algorithm and its application on structural design, *Adv Sci Lett*, 2011; **4** (3): 900-905.
19. Zhong GQ, Liu F. Discrete variable optimization of plate structures using group search optimizers, *Adv Sci Lett*, 2011; **4**(3):1057-1061.
20. Liu F, Li LJ, Yuan B. Multi-objective optimal design of frame structures with group search optimizer, *The third International Symposium on Computational Mechanics (ISCM III) in conjunction with the second symposium on Computational Structural Engineering (CSE II)* December, Taipei. 2011, pp. 968-975.
21. Rechiand Y, Fung K, Tang JF, et al. Extension of a hybrid genetic algorithm for nonlinear programming problems with equality and inequality constraints, *Comput Oper Res*, 2002; **29**: 261-274.
22. Zheng JH. *Multi-objective evolutionary algorithm and its application*, Science Press, Beijing, 2007.